

Shadow of axisymmetric, stationary and asymptotically flat black holes in the presence of plasma

Javier Badía^{1,2*}, Ernesto F. Eiroa^{1†}

¹ Instituto de Astronomía y Física del Espacio (IAFE, CONICET-UBA),
Casilla de Correo 67, Sucursal 28, 1428, Buenos Aires, Argentina

² Departamento de Física, Facultad de Ciencias Exactas y Naturales,
Universidad de Buenos Aires, Ciudad Universitaria Pabellón I, 1428, Buenos Aires, Argentina

Abstract

We study the shadow produced by a class of rotating black holes surrounded by plasma. The metric for these black holes arises by applying the Newman-Janis algorithm to a family of spherically symmetric spacetimes, which includes several well known geometries as special cases. We find a general expression for the shape of the shadow in the case that the plasma frequency leads to a separable Hamilton-Jacobi equation. We present examples of the shadow contours and the observables obtained from them, for Kerr-Newman-like and 4D Einstein-Gauss-Bonnet gravity spacetimes.

1 Introduction

Two years ago, the international collaboration Event Horizon Telescope (EHT) announced the first reconstructed image [1] of the supermassive black hole at the center of the giant elliptical galaxy M87 [2], which shows the shadow surrounded by the light coming from the accretion disk around M87*; the observed bright emission ring has a diameter of $42 \pm 3 \mu\text{as}$. This telescope consists of a very long baseline interferometry (VLBI) array of instruments spread over the Earth, operating in millimeter radio waves (230 GHz). The shadow of the supermassive black hole Sgr A* at the center of the Milky Way [3] is also of interest for this kind of observation, but it has not been fully achieved yet. The shadow or apparent shape of a black hole —as seen by a far away observer— is a consequence of the particular behavior of the photons in the vicinity of these compact objects. In the case of a non-rotating black hole it has the shape of a circle, while rotating ones present a deformation that increases with the spin [4, 5]. Many articles have been published on this topic in the years previous to the EHT discovery, both in Einstein theory [6–9] and in modified gravity [10–14]. In general relativity, the size and the shape of the shadow depend on the mass, the angular momentum and the inclination angle of the black hole, along with other variables that can appear due to the presence of matter or fields; while in modified gravity they can also depend on other parameters related to the particular theory adopted. There has been a surge in the number of articles published on this topic since the EHT discovery; we can mention [15–21] among them. For an up to date review of analytical studies see [22]. Interesting discussions about the physical nature of the black hole photon ring and the shadow have recently appeared in the literature [23]. The study of black hole shadows can be a useful tool for a better understanding of astrophysical

*e-mail: jbadia@iafe.uba.ar

†e-mail: eiroa@iafe.uba.ar

black holes at the center of galaxies. The measurement of black hole shadows has been proposed for testing general relativity in the strong field regime, allowing for a comparison with other theories of gravity [24]. An improvement in the observations by the EHT is expected in the coming years, which would lead to a more detailed picture of M87* and also to the acquisition of images of other nearby supermassive black holes [25–28].

The presence of plasma surrounding an astrophysical object results in a change of the trajectories of light rays with respect to those in a vacuum background. But plasma is also a dispersive medium, so photons with different frequencies follow distinct trajectories; as a consequence, the optical properties are chromatic. In the context of geometrical optics, the plasma can be considered as a dispersive medium characterized by an index of refraction depending on the frequency. One particular aspect that has been analyzed in recent years is the influence of plasma on the shadow of black holes, both in the spherically symmetric [29] and in the rotating [30–34] cases. In this article, we investigate the shadow cast by a class of rotating black holes surrounded by plasma, which results from applying the Newman-Janis algorithm to spherically symmetric spacetimes. We obtain a general expression for the contour of the shadow when the plasma frequency leads to a separable Hamilton-Jacobi equation. We present examples corresponding to Kerr-Newman-like and 4D Einstein-Gauss-Bonnet theory black holes, for which we introduce and calculate the observables. The paper is organized as follows. In Sec. 2, we separate the Hamilton-Jacobi equation in the case of photons in plasma. In Sec. 3, we find the contour of the shadow. In Sec. 4, we show the examples. Finally, in Sec. 5, we discuss the main results. We adopt units such that $G = c = 1$.

2 Hamilton-Jacobi equation for light rays in a plasma

The motion of photons in a pressureless, nonmagnetized plasma is governed by the Hamiltonian [35, 36]

$$\mathcal{H} = \frac{1}{2} (g^{\mu\nu}(x)p_\mu p_\nu + \omega_p(x)^2), \quad (1)$$

where $g^{\mu\nu}$ is the inverse spacetime metric and ω_p is the plasma electron frequency, given by

$$\omega_p^2 = \frac{4\pi e^2}{m_e} N, \quad (2)$$

with e and m_e the electron charge and mass respectively, and N the electron number density. We assume that both the metric and the plasma frequency are stationary and axisymmetric, so that neither the components $g_{\mu\nu}$ nor ω_p can depend on the Boyer-Lindquist coordinates t and φ . Since $\mathcal{H} = 0$ for a light ray, the form of the Hamiltonian implies that light in the presence of plasma follows timelike worldlines for the metric $g_{\mu\nu}$. A given ω_p also fixes the normalization of the curve parameter, with the Cartesian components of the four-momentum having units of frequency. For this reason, we will follow Ref. [31] and use the name $\omega_0 \equiv -p_t$ for the conserved quantity commonly named “energy”. Note, however, that in our definition ω_0 is positive for a future directed vector, since we are interested in future directed rather than past directed rays. Another consequence of the presence of plasma is the existence of forbidden regions, where light rays cannot exist. The analysis carried out in Ref. [31] for the Kerr spacetime can be straightforwardly generalized to an arbitrary stationary, axisymmetric and asymptotically flat metric, with the result that

$$\omega_0^2 \geq -g_{tt}\omega_p^2 \quad (3)$$

is a necessary and sufficient condition for at least one light ray with a given frequency ω_0 to exist at a given spacetime point.

We now specialize to our chosen line element [14], given in Boyer-Lindquist coordinates by

$$ds^2 = -\frac{\rho^2 \Delta}{\Sigma} dt^2 + \frac{\Sigma \sin^2 \theta}{\rho^2} \left[d\varphi - \frac{2am(r)r}{\Sigma} dt \right]^2 + \frac{\rho^2}{\Delta} dr^2 + \rho^2 d\theta^2, \quad (4)$$

where

$$\rho^2 = r^2 + a^2 \cos^2 \theta, \quad (5)$$

$$\Delta = r^2 - 2m(r)r + a^2, \quad (6)$$

$$\Sigma = (r^2 + a^2)^2 - a^2 \Delta \sin^2 \theta. \quad (7)$$

Here $m(r)$ is a function that approaches the mass M of the black hole as $r \rightarrow \infty$, and $a = J/M$ is the angular momentum per unit mass of the black hole. The metric (4) arises by applying the Newman-Janis algorithm [14, 37] to a spherically symmetric seed metric of the form

$$ds^2 = -\left(1 - \frac{2m(r)}{r}\right) dt^2 + \frac{dr^2}{1 - 2m(r)/r} + r^2(d\theta^2 + \sin^2 \theta d\varphi^2). \quad (8)$$

In order that the geometry (4) represents a rotating black hole, we assume that the equation $\Delta(r) = 0$ has one or more positive solutions, the largest of which is the event horizon. It is easily seen that this spacetime is asymptotically flat, stationary and axisymmetric, and therefore the quantities $p_t = -\omega_0$ and p_φ are conserved along geodesics; since ω_p is a function only of the r and θ coordinates, these quantities will still be conserved in the presence of plasma.

To find one more conserved quantity and bring the equations of motion to first-order form, we write down the Hamilton-Jacobi equation

$$\mathcal{H}\left(x, \frac{\partial S}{\partial x}\right) + \frac{\partial S}{\partial \lambda} = 0, \quad (9)$$

where λ is the affine parameter along the curve, and attempt to separate variables with the ansatz

$$S = -\omega_0 t + p_\varphi \varphi + S_r(r) + S_\theta(\theta). \quad (10)$$

Substituting into Eq. (9) and setting $\mathcal{H} = 0$ as appropriate for a light ray, we arrive at

$$\begin{aligned} \Delta(S'_r)^2 - \frac{1}{\Delta} [(r^2 + a^2)^2 \omega_0^2 + 4amr\omega_0 p_\varphi + a^2 p_\varphi^2] + \\ + (S'_\theta)^2 + a^2 \omega_0^2 \sin^2 \theta + \frac{p_\varphi^2}{\sin^2 \theta} + \rho^2 \omega_p^2 = 0, \end{aligned} \quad (11)$$

where the prime denotes the derivative with respect to r or θ , as appropriate. It can be seen, as previously shown for the Kerr spacetime [31], that the equation is separable if and only if the plasma frequency can be written in the form

$$\omega_p^2 = \frac{f_r(r) + f_\theta(\theta)}{\rho^2}, \quad (12)$$

with f_r and f_θ arbitrary functions of their respective coordinates. We take the plasma frequency to be of this form from now on. By substituting this expression for ω_p into the Hamilton-Jacobi equation (11), we can separate it as

$$(S'_\theta)^2 + \left(a\omega_0 \sin \theta - \frac{p_\varphi}{\sin \theta}\right)^2 + f_\theta = -\Delta(S'_r)^2 + \frac{1}{\Delta} [\omega_0(r^2 + a^2) - ap_\varphi]^2 - f_r. \quad (13)$$

Since the left hand side is a function only of θ and the right hand side a function only of r , they must both be equal to a constant \mathcal{K} . For future convenience, we use instead Carter's constant [38], defined by $\mathcal{Q} = \mathcal{K} - (p_\varphi - a\omega_0)^2$.

From Hamilton's equations, the derivatives of the t and φ coordinates can be found from $\dot{x}^\mu = g^{\mu\nu}p_\nu$, where the dot represents the derivative with respect to λ . By setting the covariant momenta equal to the derivatives of S , the equations of motion can then be brought to the first-order ones:

$$\rho^2 \dot{t} = \frac{r^2 + a^2}{\Delta} P(r) - a(a\omega_0 \sin^2 \theta - p_\varphi), \quad (14)$$

$$\rho^2 \dot{\varphi} = \frac{a}{\Delta} P(r) - a\omega_0 + \frac{p_\varphi}{\sin^2 \theta}, \quad (15)$$

$$\rho^2 \dot{r} = \pm \sqrt{R(r)}, \quad (16)$$

$$\rho^2 \dot{\theta} = \pm \sqrt{\Theta(\theta)}, \quad (17)$$

where

$$R(r) = P(r)^2 - \Delta[\mathcal{Q} + (p_\varphi - a\omega_0)^2 + f_r], \quad (18)$$

$$\Theta(\theta) = \mathcal{Q} + \cos^2 \theta \left(a^2 \omega_0^2 - \frac{p_\varphi^2}{\sin^2 \theta} \right) - f_\theta, \quad (19)$$

$$P(r) = \omega_0(r^2 + a^2) - ap_\varphi. \quad (20)$$

We have finally arrived at the equations of motion for photons in a spacetime of the form (4) in the presence of plasma. After a suitable identification of the metric functions, it is straightforward to verify that our results agree with those obtained in Ref. [34].

3 Photon orbits and the shadow of the black hole

We are now interested in finding the spherical photon orbits, defined as the null geodesics that stay at a constant value of r . These trajectories will serve as the limiting case for the rays that form the boundary of the black hole shadow.

3.1 Spherical photon orbits

Finding the trajectories with constant r is, from the radial equation of motion, equivalent to obtaining solutions to the simultaneous equations $R(r) = R'(r) = 0$. We assume that such solutions exist and that they are unstable, satisfying $R''(r) > 0$. We follow the standard method, described for example in Ref. [14], for the calculation of the constants of motion p_φ and \mathcal{Q} in terms of the radius r of the spherical photon orbit. From the equation $R(r) = 0$ we can easily solve for \mathcal{Q} :

$$\mathcal{Q} + (p_\varphi - a\omega_0)^2 + f_r = \frac{(\omega_0(r^2 + a^2) - ap_\varphi)^2}{\Delta}. \quad (21)$$

Then replacing into $R'(r) = 0$, we have

$$R' = 4\omega_0 r (\omega_0(r^2 + a^2) - ap_\varphi) - \frac{\Delta'}{\Delta} (\omega_0(r^2 + a^2) - ap_\varphi)^2 - \Delta f'_r = 0, \quad (22)$$

which is a quadratic equation for p_φ , with solution

$$\frac{ap_\varphi}{\omega_0} = r^2 + a^2 - \frac{2r\Delta}{\Delta'} \left(1 \pm \sqrt{1 - \frac{\Delta' f'_r}{4\omega_0^2 r^2}} \right). \quad (23)$$

Finally, this equation has to be replaced in Eq. (21) to solve for \mathcal{Q} as a function of r . A possibly helpful intermediate step is to use Eq. (22) to arrive at the relation

$$\frac{\Delta'}{\Delta} a^2 (p_\varphi - a\omega_0)^2 = 2a\omega_0 r \left(\frac{r\Delta'}{\Delta} - 2 \right) (p_\varphi - a\omega_0) + 4\omega_0^2 r^3 - \frac{\Delta'}{\Delta} \omega_0^2 r^4 - \Delta f'_r, \quad (24)$$

so that one does not have to calculate the square of $p_\varphi - a\omega_0$. Putting all together, we get

$$\mathcal{Q} = -\frac{\omega_0^2 r^4}{a^2} + \frac{4\omega_0^2 r^2 \Delta}{a^2 \Delta'} \left[r - \frac{2}{\Delta'} (\Delta - a^2) \right] \left(1 \pm \sqrt{1 - \frac{\Delta' f'_r}{4\omega_0^2 r^2}} \right) + \frac{\Delta f'_r}{\Delta' a^2} (\Delta - a^2) - f_r. \quad (25)$$

For a radius r and a frequency ω_0 , Eqs. (23) and (25) give the critical values of the conserved quantities p_φ and \mathcal{Q} associated with the corresponding spherical orbit. From Eq. (17) we see that any trajectory must have $\Theta \geq 0$. If for a fixed r we then replace the critical values of p_φ and \mathcal{Q} into the inequality $\Theta \geq 0$, we arrive at

$$\mathcal{Q}(r) + \cos^2 \theta \left(a^2 \omega_0^2 - \frac{p_\varphi(r)^2}{\sin^2 \theta} \right) - f_\theta(\theta) \geq 0, \quad (26)$$

where $\mathcal{Q}(r)$ and $p_\varphi(r)$ are given by Eqs. (23) and (25). The region defined by Eq. (26) is known as the photon region, and spherical photon orbits exist at values of r and θ for which this inequality is satisfied. The range of possible radii in Eqs. (23) and (25) consists of those values of r for which there exists at least one value of θ satisfying Eq. (26).

3.2 Black hole shadow

For a far away observer, the black hole shadow is the set of directions in the sky which when propagated backwards in time never reach infinity, and instead cross the event horizon. Its boundary consists of those rays that asymptotically approach the spherical photon orbits of the spacetime, and which therefore have the same conserved quantities as them. To relate directions in the sky to the constants of motion of the light ray, we take an observer at $\theta = \theta_o$ in the asymptotically flat region and construct the orthonormal tetrad [14]

$$\mathbf{e}_{(0)} = \partial_t, \quad (27)$$

$$\mathbf{e}_{(1)} = \partial_r, \quad (28)$$

$$\mathbf{e}_{(2)} = \frac{1}{r} \partial_\theta, \quad (29)$$

$$\mathbf{e}_{(3)} = \frac{1}{r \sin \theta_o} \partial_\varphi, \quad (30)$$

so that the orthonormal components of the four-momentum are given by

$$p^{(0)} = \omega_0, \quad (31)$$

$$p^{(1)} = p^r, \quad (32)$$

$$p^{(2)} = r p^\theta, \quad (33)$$

$$p^{(3)} = \frac{p_\varphi}{r \sin \theta_o}. \quad (34)$$

We also define the norm of the spatial momentum

$$p = \left(\sum_{i=1}^3 p^{(i)} p^{(i)} \right)^{1/2}. \quad (35)$$

From the condition that the Hamiltonian (1) equal zero for a light ray, we find that $p^2 = \omega_0^2 - \omega_\infty^2$, where ω_∞^2 is the limiting value of ω_p^2 as $r \rightarrow \infty$. Note that ω_∞^2 is finite if and only if f_r goes as r^2 as $r \rightarrow \infty$, in which case we have

$$\omega_\infty^2 = \lim_{r \rightarrow \infty} \frac{f_r(r)}{r^2}. \quad (36)$$

We then adopt the celestial coordinates for an observer at infinity

$$\alpha = -r_0 \frac{p^{(3)}}{p} \Big|_{r_0 \rightarrow \infty}, \quad (37)$$

$$\beta = -r_0 \frac{p^{(2)}}{p} \Big|_{r_0 \rightarrow \infty}, \quad (38)$$

and insert the expression (17) for p^θ as a function of the conserved quantities to finally arrive at

$$\alpha = -\frac{p_\varphi}{\sqrt{\omega_0^2 - \omega_\infty^2} \sin \theta_o}, \quad (39)$$

$$\beta = \pm \frac{1}{\sqrt{\omega_0^2 - \omega_\infty^2}} \sqrt{\mathcal{Q} + \cos^2 \theta_o \left(a^2 \omega_0^2 - \frac{p_\varphi^2}{\sin^2 \theta_o} \right) - f_\theta(\theta_o)}. \quad (40)$$

For a given ω_0 , the contour of the black hole shadow is described by a parametric curve $(\alpha(r), \beta(r))$, with p_φ and \mathcal{Q} given as functions of r by Eqs. (23) and (25), and r bounded in the region $r_+ \leq r \leq r_-$, with r_\pm the values for which $\beta(r_\pm) = 0$. Comparing with Eq. (26), this is the intersection of the photon region with the cone $\theta = \theta_o$. Note also that the functions $\alpha(r)$ and $\beta(r)$ depend on the frequency ω_0 only through the ratio ω_p/ω_0 .

3.3 Observables

Following our previous work [21], in addition to the shadow contour we calculate three observables: the area of the black hole shadow, its oblateness, and the horizontal displacement of its centroid [8, 18, 21]. The area is simply defined as

$$A = 2 \int \beta d\alpha = 2 \int_{r_+}^{r_-} \beta(r) |\alpha'(r)| dr, \quad (41)$$

with the factor of two arising from the up-down symmetry of the shadow, since the curve $(\alpha(r), \beta(r))$ only describes half of the contour. The oblateness is related to the deformation of the shadow as compared to a circle, and is defined as

$$D = \frac{\Delta\alpha}{\Delta\beta}, \quad (42)$$

where $\Delta\alpha$ and $\Delta\beta$ are the horizontal and vertical extent of the shadow respectively; the Kerr shadow has $D < 1$, with $D = 1$ for the limiting case of a circle. Finally, the horizontal coordinate of the centroid is given by

$$\alpha_c = \frac{2}{A} \int \alpha\beta d\alpha = \frac{2}{A} \int_{r_+}^{r_-} \alpha(r)\beta(r) |\alpha'(r)| dr, \quad (43)$$

with the same factor of two as in the definition of the area.

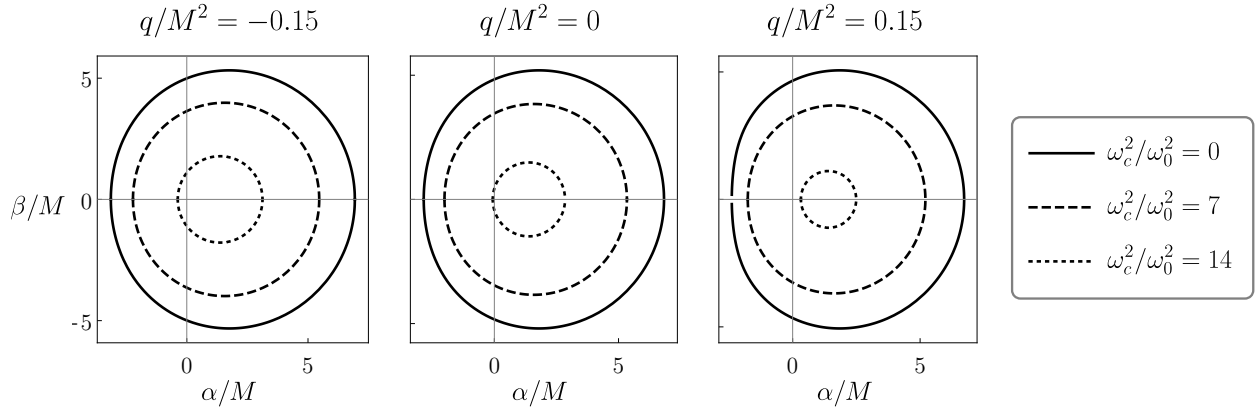


Figure 1: Shadow of a Kerr-Newman-like black hole with spin $a/M = 0.9$ surrounded by a Shapiro-type plasma distribution with $f_r(r) = \omega_c^2 \sqrt{M^3 r}$, as viewed by an equatorial observer.

4 Examples

In this section, we obtain the contour of the shadow for various black hole metrics, using the formalism described in Sec. 3, and we calculate the three observables defined in the previous section as functions of the parameters of each example, as a way to characterize their size and shape. As our model of plasma, we adopt the well known case of dust that is at rest at infinity, first considered by Shapiro [39]. In the Kerr spacetime the mass density, and by Eq. (2) the squared plasma frequency, go as $r^{-3/2}$, being independent of θ to a very good approximation¹. However, such a plasma distribution cannot be put into the separable form given by Eq. (12); therefore, following Ref. [31] we take the frequency to have an additional θ dependency by choosing

$$f_r(r) = \omega_c^2 \sqrt{M^3 r}, \quad (44)$$

$$f_\theta(\theta) = 0, \quad (45)$$

so that

$$\omega_p^2 = \omega_c^2 \frac{\sqrt{M^3 r}}{r^2 + a^2 \cos^2 \theta}, \quad (46)$$

where ω_c is a constant and M is the mass of the black hole; as mentioned in Sec. 3.2, the photon trajectories with a given frequency ω_0 depend only on the ratio ω_c/ω_0 . At large distances from the black hole, the metrics considered here approach the Kerr metric as long as we have $m(r) \rightarrow M$, so we expect that the Shapiro solution is still valid. At small distances the chosen metric may be quite different from the Kerr metric, so we will work under the assumption that the plasma density (46) is not significantly affected.

4.1 Kerr-Newman-like black hole

As our first example, we take the metric given by the function

$$m(r) = M - \frac{q}{2r}, \quad (47)$$

with M a positive constant representing the mass of the black hole and q an arbitrary real constant. If q is positive and we set $q = Q^2$, the resulting metric is that of the Kerr-Newman spacetime with

¹The density actually goes to a constant at infinity, with $\rho \sim r^{-3/2}$ only being true at distances below the capture radius of the black hole. We consider the density at infinity to be negligible, and take $\rho \propto r^{-3/2}$ everywhere.

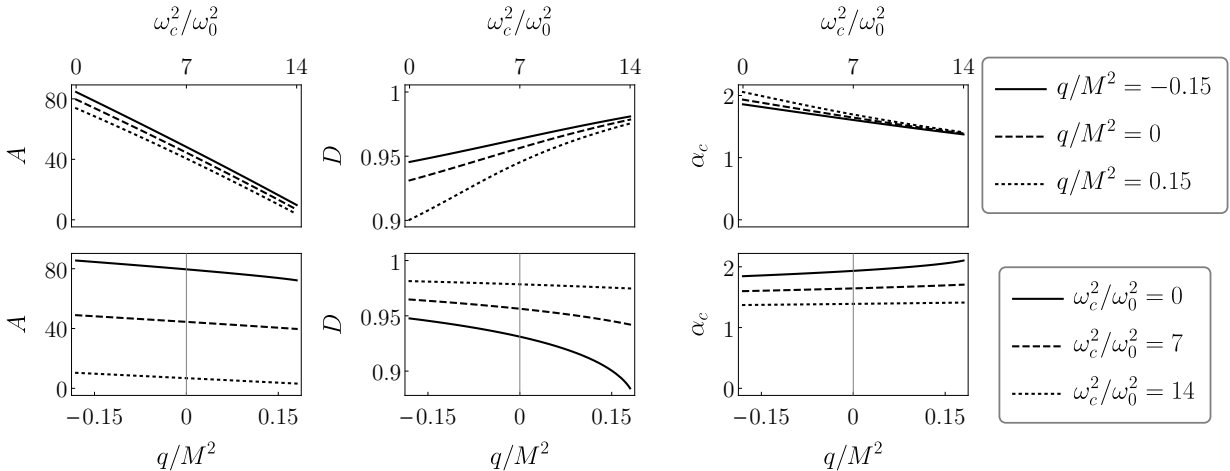


Figure 2: The area (A), the oblateness (D), and the centroid (α_c) of the shadow of a Kerr-Newman-like black hole with spin $a/M = 0.9$ in a Shapiro-type plasma, as viewed by an equatorial observer. *Top*: The three observables as functions of the photon frequency for three values of the charge q . *Bottom*: The three observables as functions of the charge for three different values of the photon frequency.

electric charge Q . However, we also allow negative values of q ; such a metric arises in the absence of the electromagnetic field in alternative theories of gravity, such as special cases of Horndeski theory [40] or within general relativity in the presence of certain matter fields. Horndeski gravity is the most general scalar tensor theory with second order derivative equations of motion, being the main theoretical framework for scalar-tensor models in which cosmological observations can be interpreted. Another interesting case arises within the Randall-Sundrum braneworld model, where q in the four dimensional black hole solution on the brane is understood as a tidal charge generated by gravitational effects coming from a fifth dimension; see for example [11] –where the shadow without the presence of plasma is analyzed– and the references therein. For that reason and in analogy with the electric charge, in the following we will use the name “charge” for it. As in the Kerr-Newman case, the inequality $a^2 + q \leq M^2$ is a necessary and sufficient condition to avoid a naked singularity, and we assume that it is satisfied.

For the plasma model adopted here, a forbidden region appears if the frequency is low enough, where the condition (3) is not satisfied. This axially symmetric region initially develops around the poles and expands towards the equator as the frequency decreases, eventually enveloping the black hole.

The contour of the shadow for a black hole with $a = 0.9M$ and some values for the photon frequency is displayed in Fig. 1, and the corresponding observables are shown in Fig. 2. It is clear from the plots that the shadow becomes smaller as the frequency decreases; it disappears entirely below a certain frequency, due to the appearance of the forbidden region. We see that overall, the dependency of the observables on the frequency is stronger than on the tidal charge, with a slight exception for the oblateness at small frequency and near-extremal charge.

4.2 4D Einstein-Gauss-Bonnet gravity black hole

Recently, a novel gravity theory was proposed by rescaling the coupling constant and taking the limit $D \rightarrow 4$ in D -dimensional Einstein-Gauss-Bonnet theory [41], thereby bypassing the standard result that four-dimensional Einstein-Gauss-Bonnet theory is purely topological and thus equivalent

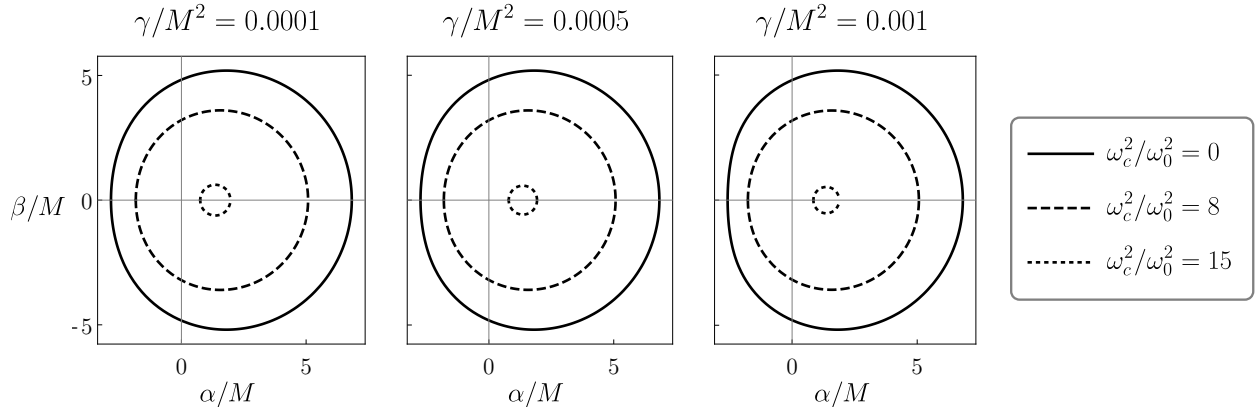


Figure 3: Shadow of a 4D Einstein-Gauss-Bonnet black hole with spin $a/M = 0.9$ surrounded by a Shapiro-type plasma distribution with $f_r(r) = \omega_c^2 \sqrt{M^3 r}$, as viewed by an equatorial observer.

to general relativity. However, the original formulation is based on some particular solutions and it lacks a complete set of four-dimensional field equations that can be written in closed form. This theory was subsequently placed on firmer ground [42], by showing that in addition to the metric tensor it propagates a scalar field and the full action belongs to the Horndeski class of scalar-tensor theories of gravity. The action is obtained by a regularization procedure in a way that is free from divergences and produces well behaved second-order field equations. The result is a new theory of gravity in four dimensions that includes a nonvanishing contribution coming from the Gauss-Bonnet term. A rotating solution was later found [43] by applying a modified version of the Newman-Janis algorithm, resulting in a metric of the form (4), with the function $m(r)$ given by

$$m(r) = \frac{r^3}{64\pi\gamma} \left(\sqrt{1 + \frac{128\pi\gamma M}{r^3}} - 1 \right), \quad (48)$$

where γ is a parameter of the theory, with units of mass squared; see Ref. [44] for a discussion of observational constraints on its value. The black hole mass is M , since we have $m(r) \rightarrow M$ as $r \rightarrow \infty$. The limit $\gamma \rightarrow 0$ corresponds to the Kerr geometry. The Newman-Janis algorithm does not guarantee that the rotating metric will be a solution of the original field equations, so an appropriate set of field equations, possibly with an unknown matter component, is assumed for this example. We will only consider positive values for γ , since the square root in Eq. (48) becomes imaginary for a finite value of r if γ is negative.

We use a spin $a/M = 0.9$ in Figs. 3 and 4, as in the previous example. In this case, by solving the equations $\Delta = \Delta' = 0$ numerically, it can be seen that the spacetime contains an event horizon if $\gamma/M^2 < 0.00129$, and there is a naked singularity for larger values of γ . Similarly to the Kerr-Newman-like black hole, when including the Shapiro-type plasma distribution a forbidden region develops as the frequency of light decreases, resulting in a dramatic decrease of the shadow size as seen in Fig. 3. This is also shown in Fig. 4, which plots the three observables as a function of the parameters. It can be seen that the overall behavior of the observables is very similar to the one obtained for the Kerr-Newman-like black hole, with a smaller variation when changing the parameter since the range of allowed values for γ is much smaller than that corresponding to the charge q .

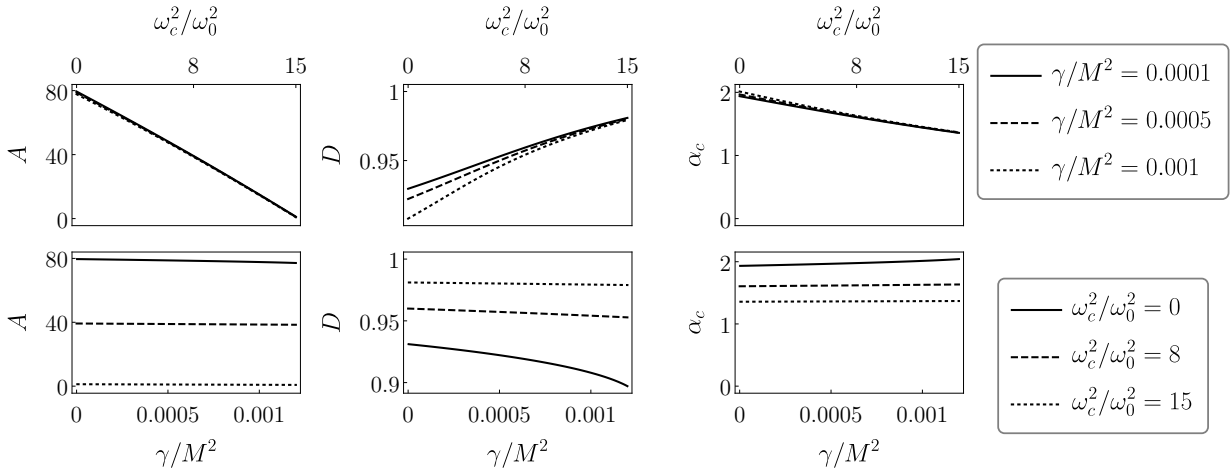


Figure 4: The area (A), the oblateness (D), and the centroid (α_c) of the shadow of a 4D Einstein-Gauss-Bonnet black hole with spin $a/M = 0.9$ in a Shapiro-type plasma, as viewed by an equatorial observer. *Top*: The three observables as functions of the photon frequency for three values of the EGB parameter γ . *Bottom*: The three observables as functions of γ for three different values of the photon frequency.

5 Conclusions

In this article, we have analyzed how the presence of plasma modifies the size and the shape of the shadow corresponding to a class of rotating black holes obtained by the Newman-Janis procedure. These spacetimes lead to a Hamilton-Jacobi equation for light rays that is always separable, as long as the plasma frequency satisfies a certain condition, as in the Kerr case [8]. The presence of plasma makes light follow timelike curves, leading to a modification of the photon regions and frequency-dependent forbidden regions, where light cannot travel. We have not considered the gravitational influence of the plasma itself, taking it to be negligible compared with that of the black hole, nor any processes of scattering, emission or absorption. These effects should be included if the goal is to produce a realistic image of the surroundings of a black hole and not only the shadow boundary.

Assuming that the plasma frequency obeys the separability condition introduced in Ref. [31], we have obtained the expressions for the celestial coordinates of the shadow contour as viewed by a far away observer. As in the Kerr case, the presence of the plasma introduces a dependency on the photon frequency through the ratio ω_p/ω_0 , and thus this dependency is relative to the frequency scale set by ω_p . The expressions for the celestial coordinates reduce to the already known ones [14] when the plasma frequency is set to zero, or equivalently when the photon frequency tends to infinity. These expressions are the central result of this paper: for a metric obtained by the Newman-Janis algorithm and a plasma distribution satisfying the separability condition, one can plot the black hole shadow as seen by an observer at infinity, given values for the observer inclination and the photon frequency. One can also calculate various observables, such as the three we have defined: the area, oblateness and centroid of the shadow. These can be contrasted with an observation of a black hole shadow by the EHT or other future instruments to test alternatives to the Kerr metric; among our observables, the displacement of the centroid is perhaps the most difficult one to determine observationally, since it requires an independent knowledge of the black hole's true position in the sky. The area scales with the black hole mass and distance, which are typically known, while the oblateness is an intrinsic geometric and scale-invariant property of the shadow.

We have also applied our results to two example geometries, considering in both cases an equatorial observer for simplicity. For our plasma distribution we have chosen a variation of the one proposed by Shapiro [39], which models dust surrounding a Kerr black hole and that is at rest at infinity. The original solution is a function of r only and thus does not obey the separability condition for the plasma density, so we have added a slight θ dependency to be able to use it within our formalism. Since we are not considering the Kerr metric but rather alternatives to it, especially at short distances, we also assume that the form of the corresponding plasma densities is not significantly altered from the original one, derived assuming a Kerr black hole. As our first example we have used a metric that we have named “Kerr-Newman-like”, since it is identical in form to the Kerr-Newman metric but allowing the squared charge to take either sign. This metric arises in various scenarios involving matter fields, alternative theories of gravity, or possible effects of extra dimensions, as previously mentioned. The second example comes from a recently proposed theory dubbed (novel) 4-dimensional Einstein-Gauss-Bonnet, first motivated by the attempt to find a nontrivial limit of D -dimensional Einstein-Gauss-Bonnet theory as $D \rightarrow 4$. The shadows in both examples are qualitatively similar, with the clearest feature being the appearance of a forbidden region around the black hole. This forbidden region starts as two caps around the poles and grows towards the equatorial plane as the frequency decreases, leading to a sharp reduction of the shadow size and its eventual disappearance.

For the supermassive black holes at the centers of the Milky Way and the galaxy M87, which are the main focus of attention of current observational efforts by the EHT, it is expected that plasma effects start to become relevant at radio wavelengths of a few centimeters or more [29]. However, present and planned instruments focus on the submillimeter range, where scattering and self-absorption do not have a significant effect on the emitted radiation in the area surrounding the black hole, so that a realistic observation of the influence of a plasma on the shadow does not seem feasible at the moment.

Acknowledgments

This work has been supported by CONICET and Universidad de Buenos Aires.

References

- [1] K. Akiyama *et al.* (Event Horizon Telescope), *Astrophys. J.* **875**, L1 (2019); **875**, L2 (2019); **875**, L3 (2019); **875**, L4 (2019); **875**, L5 (2019); **875**, L6 (2019).
- [2] A.E. Broderick, R. Narayan, J. Kormendy, E.S. Perlman, M.J. Rieke, and S.S. Doeleman, *Astrophys. J.* **805**, 179 (2015).
- [3] S. Gillessen *et al.*, *Astrophys. J.* **837**, 30 (2017).
- [4] J. Bardeen, *Black Holes*, Proceedings of École d’été de Physique Théorique, Les Houches 1972, 215-240, edited by C. De Witt and B.S. De Witt (Gordon and Breach Science Publishers, New York, 1973).
- [5] S. Chandrasekhar, *The Mathematical Theory of Black Holes* (Oxford University Press, New York, 1992).
- [6] J.P. Luminet, *Astron. Astrophys.* **75**, 228 (1979); H. Falcke, F. Melia, and E. Agol, *Astrophys. J.* **528**, L13 (2000); A. de Vries, *Class. Quantum Grav.* **17**, 123 (2000).

- [7] R. Takahashi, *Astrophys. J.* **611**, 996 (2004); C. Bambi and K. Freese, *Phys. Rev. D* **79**, 043002 (2009); K. Hioki and K.I. Maeda, *Phys. Rev. D* **80**, 024042 (2009); N. Tsukamoto, Z. Li, and C. Bambi, *JCAP* 06 (2014) 043.
- [8] O.Y. Tsupko, *Phys. Rev. D* **95**, 104058 (2017).
- [9] G.S. Bisnovatyi-Kogan and O.Y. Tsupko, *Phys. Rev. D* **98**, 084020 (2018); X. Hou, Z. Xu and J. Wang, *JCAP* 12 (2018) 040.
- [10] K. Hioki and U. Miyamoto, *Phys. Rev. D* **78**, 044007 (2008); L. Amarilla, E.F. Eiroa, and G. Giribet, *Phys. Rev. D* **81**, 124045 (2010); L. Amarilla and E.F. Eiroa, *Phys. Rev. D* **87**, 044057 (2013).
- [11] J. Schee and Z. Stuchlik, *Int. J. Mod. Phys. D* **18**, 983 (2009); L. Amarilla and E.F. Eiroa, *Phys. Rev. D* **85**, 064019 (2012).
- [12] A. Grenzebach, V. Perlick, and C. Lämmerzahl, *Phys. Rev. D* **89**, 124004 (2014); E.F. Eiroa and C.M. Sendra, *Eur. Phys. J. C* **78**, 91 (2018); A. Övgün, I. Sakalli, and J. Saavedra, *JCAP* 10 (2018) 041.
- [13] P.V.P. Cunha, C.A.R. Herdeiro, E. Radu, and H.F. Runarsson, *Phys. Rev. Lett.* **115**, 211102 (2015); F. H. Vincent, E. Gourgoulhon, C. Herdeiro, and E. Radu, *Phys. Rev. D* **94**, 084045 (2016); M. Amir and S.G. Ghosh, *Phys. Rev. D* **94**, 024054 (2016); Z. Younsi, A. Zhidenko, L. Rezzolla, R. Konoplya, and Y. Mizuno, *Phys. Rev. D* **94**, 084025 (2016) P.V.P. Cunha and C.A.R. Herdeiro, *Gen. Relativ. Gravit.* **50**, 42 (2018).
- [14] N. Tsukamoto, *Phys. Rev. D* **97**, 064021 (2018).
- [15] K. Jusufi, M. Jamil, P. Salucci, T. Zhu, and S. Haroon, *Phys. Rev. D* **100**, 044012 (2019); C. Bambi, K. Freese, S. Vagnozzi, and L. Visinelli, *Phys. Rev. D* **100**, 044057 (2019); J.C.S. Neves, *Eur. Phys. J. C* **80**, 717 (2020).
- [16] R.A. Konoplya, *Phys. Lett. B* **795**, 1 (2019); S. Vagnozzi and L. Visinelli, *Phys. Rev. D* **100**, 024020 (2019); R. Kumar, S.G. Ghosh, and A. Wang, *Phys. Rev. D* **100**, 124024 (2019); F. Long, J. Wang, S. Chen, and J. Jing, *JHEP* 10 (2019) 269.
- [17] R. Shaikh, *Phys. Rev. D* **100**, 024028 (2019).
- [18] R. Kumar and S.G. Ghosh, *Astrophys. J.* **892**, 78 (2020).
- [19] O.Y. Tsupko, Z. Fan, and G.S. Bisnovatyi-Kogan, *Class. Quantum Grav.* **37**, 065016 (2020); Z. Chang and Q. Zhu, *Phys. Rev. D* **101**, 084029 (2020); E. Contreras, A. Rincón, G. Pantopoulos, P. Bargueño, and B. Koch, *Phys. Rev. D* **101**, 064053 (2020); P.-C. Li, M. Guo, and B. Chen, *Phys. Rev. D* **101**, 084041 (2020).
- [20] I. Banerjee, S. Chakraborty, and S. SenGupta, *Phys. Rev. D* **101**, 041301(R) (2020); M. Khodadi, A. Allahyari, S. Vagnozzi, and D.F. Mota, *JCAP* **09**, 026 (2020); Z. Hu, Zhen Zhong, P.C. Li, M. Guo, and B. Chen, *Phys. Rev. D* **103**, 044057 (2021); B.H. Lee, W. Lee, and Y.S. Myung, arXiv:2101.04862 [gr-qc].
- [21] J. Badía and E.F. Eiroa, *Phys. Rev. D* **102**, 024066 (2020).
- [22] V. Perlick and O.Y. Tsupko, arXiv:2105.07101 [gr-qc].

- [23] S.E. Gralla, D.E. Holz, and R.M. Wald, Phys. Rev. D **100**, 024018 (2019); M.D. Johnson *et al.*, Sci. Adv. **6**, eaaz1310 (2020); E. Himwich, M.D. Johnson, A. Lupsasca, and A. Strominger, Phys. Rev. D **101**, 084020 (2020); S.E. Gralla and A. Lupsasca, Phys. Rev. D **101**, 044032 (2020); A. Chael, M.D. Johnson, and A. Lupsasca, arXiv:2106.00683 [astro-ph.HE].
- [24] D. Psaltis *et al.* (EHT Collaboration), Phys. Rev. Lett. **125**, 141104 (2020); S.E. Gralla, A. Lupsasca, and D.P. Marrone, Phys. Rev. D **102**, 124004 (2020); S.E. Gralla, Phys. Rev. D **103**, 024023 (2021); S.H. Völkel, E. Barausse, N. Franchini, and A.E. Broderick, arXiv:2011.06812 [gr-qc].
- [25] H. Falcke and S.B. Markoff, Class. Quantum Grav. **30**, 244003 (2013); N.S. Kardashev *et al.*, Phys. Usp. **57**, 1199 (2014); T. Johannsen, Class. Quantum Grav. **33**, 113001 (2016); C. Bambi, Rev. Mod. Phys. **89**, 025001 (2017).
- [26] Z. Zhu, M.D. Johnson, and R. Narayan, Astrophys. J. **870**, 6 (2019).
- [27] P.B. Ivanov *et al.*, Phys. Usp. **62**, 423 (2019); E. Mikheeva, S. Repin, and V. Lukash, Astron. Rep. **64**, 578 (2020).
- [28] F. Roelofs *et al.*, Astron. Astrophys. **625**, A124 (2019); C.M. Fromm, Y. Mizuno, Z. Younsi, H. Olivares, O. Porth, M. De Laurentis, H. Falcke, M. Kramer, and L. Rezzolla, Astron. Astrophys. **649**, A116 (2021).
- [29] V. Perlick, O.Y. Tsupko, and G.S. Bisnovatyi-Kogan, Phys. Rev. D **92**, 104031 (2015); O.Y. Tsupko, Phys. Rev. D **103**, 104019 (2021).
- [30] F. Atamurotov, B. Ahmedov, and A. Abdujabbarov, Phys. Rev. D **92**, 084005 (2015).
- [31] V. Perlick and O.Y. Tsupko, Phys. Rev. D **95**, 104003 (2017).
- [32] G.S. Bisnovatyi-Kogan and O.Y. Tsupko, Universe **3**, 57 (2017).
- [33] Y. Huang, Y.P. Dong, and D.J. Liu, Int. J. Mod. Phys. D **27**, 1850114 (2018); G.Z. Babar, A.Z. Babar, and F. Atamurotov, Eur. Phys. J. C **80**, 761 (2020); A. Chowdhuri and A. Bhattacharyya, arXiv:2012.12914 [gr-qc].
- [34] H.C.D. Lima Junior, L.C.B. Crispino, P.V.P. Cunha, and C.A.R. Herdeiro, Eur. Phys. J. C **80**, 1036 (2020).
- [35] J. L. Synge, *Relativity: The General Theory* (North-Holland, Amsterdam, 1960).
- [36] V. Perlick, *Ray Optics, Fermat's Principle and Applications to General Relativity* (Springer, Heidelberg, 2000).
- [37] C. Bambi and L. Modesto, Phys. Lett. B **721**, 329 (2013).
- [38] B. Carter, Phys. Rev. **174**, 1159 (1968).
- [39] S. Shapiro, Astrophys. J **189**, 343 (1974).
- [40] E. Babichev, C. Charmousis, and A. Lehébel, JCAP **04** (2017) 027.
- [41] D. Glavan and C. Lin, Phys. Rev. Lett. **124**, 081301 (2020).

- [42] P.G.S. Fernandes, P. Carrilho, T. Clifton, and D.J. Mulryne, Phys. Rev. D **102**, 024025 (2020); R.A. Hennigar, D.Kubizňák, R.B. Mann, and C. Pollack, JHEP 07 (2020) 027.
- [43] S. Wei and Y. Liu, Eur. Phys. J. Plus **136**, 436 (2021); R. Kumar and S.G. Ghosh, JCAP 07 (2020) 053.
- [44] T. Clifton, P. Carrilho, P.G.S. Fernandes, and D.J. Mulryne, Phys. Rev. D **102**, 084005 (2020).
- [45] D. Hansen and N. Yunes, Phys. Rev. D **88**, 104020 (2013).